Acta Biochim Biophys Sin 2023, 55(3): 438–448
https://doi.org/10.3724/abbs.2022178
Advance Access Publication Date: 9 December 2022
Original Article

Original Article

circ-BPTF serves as a miR-486-5p sponge to regulate CEMIP and promotes hypoxic pulmonary arterial smooth muscle cell proliferation in COPD

Changguo Wang[1,†], Yingying Liu[2,3,†], Weiyun Zhang[1,2,3], Jian'an Huang[1], Junhong Jiang[2,3,*], Ran Wang[4,*], and Daxiong Zeng[2,3,*]

[1]Department of Pulmonary and Critical Care Medicine, the First Affiliated Hospital of Soochow University, Suzhou 215006, China, [2]Department of Pulmonary and Critical Care Medicine, Suzhou Dushu Lake Hospital, Suzhou 215006, China, [3]Department of Pulmonary and Critical Care Medicine, Dushu Lake Hospital Affiliated to Soochow University, Medical Center of Soochow University, Suzhou 215006, China, and [4]Department of Respiratory and Critical Care Medicine, the First Affiliated Hospital of Anhui Medical University, Hefei 230022, China

[†]These authors contributed equally to this work.

*Correspondence address. Tel: +86-512-65955392; E-mail: zengdaxiong@suda.edu.cn (D.Z.) / E-mail: ranwangtjmu@hotmail.com (R.W.) / E-mail: jiang20001969@163.com (J.J.)

Received 18 March 2022 Accepted 2 September 2022

Abstract

Hypoxia plays a crucial role in pulmonary vascular remodelling at the early stage of chronic obstructive pulmonary disease (COPD). Circle RNA (circRNA) has been identified to play a critical role in multiple diseases. However, the role of circRNAs in pulmonary vascular remodelling in COPD remains unclear. In this study, we aim to investigate the role of circRNAs in pulmonary arterial smooth muscle cell proliferation and pulmonary vascular remodelling in COPD. COPD patients show lower partial pressure of arterial oxygen and pulmonary arterial remodeling as compared with controls. circRNA microarray and real-time PCR analyses show significantly higher level of circ-BPTF and lower miR-486-5p level in the pulmonary arteries of COPD patients as compared with controls. Hypoxia suppresses miR-486-5p expression but promotes expressions of circ-BPTF and cell migration inducing protein (CEMIP) in human pulmonary arterial smooth muscle cells (PASMCs) *in vitro*. Loss- and gain-of-function experiments show that circ-BPTF promotes PASMC proliferation *in vitro*. Moreover, luciferase reporter assay results indicate that circ-BPTF regulates PASMC proliferation by acting as an miR-486-5p sponge. *CEMIP* is identified as a candidate target gene of miR-486-5p by luciferase reporter assay. Overall, our study shows that circ-BPTF serves as a miR-486-5p sponge to regulate CEMIP and promote hypoxic PASMC proliferation in pulmonary vascular remodelling in COPD.

Key words pulmonary vascular remodelling, hypoxia, chronic obstructive pulmonary disease (COPD), circ-BPTF, miR-486-5p, CEMIP

Introduction

As a serious and progressive pulmonary vascular disease, pulmonary hypertension (PH) is a complication of multiple chronic lung diseases [1]. PH is characterized by elevated pulmonary arterial pressure and pulmonary vascular resistance, which are mainly caused by pulmonary vasoconstriction and pulmonary vascular remodelling [2]. Chronic obstructive pulmonary disease (COPD) is one of the most common disorders of the respiratory system and eventually leads to hypoxic PH [3]. Previous reports, including our studies, have proven that pulmonary vascular remodelling occurs in the early stage of COPD [4–7]. We also revealed that cyclin D1 and NR4A3 are involved in pulmonary vascular remodelling of COPD [5–9].

Although an increasing number of studies have demonstrated the role of multiple growth factors or pathways (such as prostacyclin, nitric oxide and endothelin, etc.) in pulmonary vascular remodelling, drugs targeting these pathways have little benefit to COPD patients with PH [10,11]. As a critical feature of pulmonary vascular remodelling, hypertrophy and proliferation of pulmonary artery smooth muscle cells (PASMCs) contribute greatly to the sustained increase in pulmonary vascular resistance and pulmonary artery pressure in PH [12,13]. Therefore, it is essential to explore the

molecular mechanisms responsible for PASMC proliferation to ameliorate pulmonary vascular remodelling.

Circle RNAs (circRNAs) are RNA molecules with covalently joined 3′- and 5′-ends formed by back-splicing events [14]. circRNAs widely exist in mammalian cells and exert biological effects at the posttranscriptional level by sponging miRNAs at response elements or miRNA-binding sites [15]. Recent reports indicated that circRNAs are involved in PH [16–20]. Circ-calm4 has been proven to promote PASMC proliferation by sponging miR-337-3p. hsa_circ_0016070 and mmu_circ_0000790 are also involved in PH by regulating PASMC proliferation. However, the function of circRNAs in pulmonary vascular remodelling of COPD has not been clearly reported.

In this study, we screened a novel circRNA, circ-BPTF, which showed increased expression in pulmonary arteries of COPD. We also explored its roles in PASMC proliferation and pulmonary vascular remodelling in COPD.

Materials and Methods

Lung tissue collection

This study was approved by the Research Ethics Committee of the First Affiliated Hospital of Soochow University and Dushu Lake Hospital Affiliated to Soochow University, and written informed consents were obtained from all subjects. Human peripheral lung samples were collected from patients who underwent pneumonectomy for lung volume reduction or pulmonary nodules from January 2016 to December 2019 in our hospital. Lung tissue samples were obtained from normal areas as far as possible from the pulmonary nodules (at least 2 cm). Peripheral lung samples or pulmonary arterial explants were inflated with 4% (w/v) paraformaldehyde for embedding in paraffin or stored at −80°C for subsequent protein extraction. Pulmonary function tests were performed before surgery in all patients. COPD was determined by the standard of pulmonary function as FEV1/FVC less than 0.7. Arterial blood samples were collected before the operation and patients were not receiving oxygen before blood sampling.

Pulmonary vascular morphometry

Paraffin-embedded peripheral lung samples were cut into multiple 5-μm-thick sections. Sections were deparaffinized and stained with hematoxylin and eosin (Beyotime, Shanghai, China) for morphometric measurements under an optical microscope (Olympus, Tokyo, Japan) as described in our previous reports [5–7]. The vessel wall thickness was expressed as a percentage of the external diameter [(external diameter − internal diameter)/external diameter × 100%]. The assessment was limited to medium and small arteries (≤500 μm diameter) with a complete circumferential smooth muscle layer. At least ten vessels were measured in each section.

Immunohistochemical analysis

Immunohistochemistry (IHC) analysis was performed according to the following procedure. The primary segment-specific antibody for α-smooth muscle actin (1:1000; Abcam) was applied to the tissue sections and incubated overnight at 4°C. The slides were incubated with goat anti-rabbit IgG horseradish peroxidase-conjugated secondary antibody (1:1000; Abcam) for 30 min at 22°C, followed by washing and incubation with diaminobenzidine (DAB; Beyotime). A light hematoxylin counterstain was performed,dehydrated, cleared, and mounted. Stained slides were photographed by an immunofluorescence microscope (Olympus, Japan, Tokyo). All these arteries were classified into three groups: nonmuscularized (25% circumference with α-actin staining), partially muscularized (25% to 75% circumference with α-actin staining) and fully muscularized (75% circumference with α-actin staining). The fully muscularized vessels were calculated and expressed as the percentage of total medium and small arteries. The assessment was limited to medium and small arteries (≤ 500 μm diameter) with a complete circumferential smooth muscle layer. At least five vessels were measured in each section.

circRNA microarray scan

Pulmonary arterial explants of lung samples were collected from the COPD group and the non-COPD group (three samples from each group). Total RNA was isolated using TRIzol reagent (Invitrogen, Carlsbad, USA) according to the manufacturer's protocol. RNA concentration determination, RNA quality control and microarray hybridization were performed according to the manufacturer's instructions of the Arraystar Super RNA Labeling kit (Arraystar, Rockville, USA). Linear RNAs were eliminated using RNase R (Epicenter, New York, USA). The enriched circRNAs were subsequently amplified and transcribed into fluorescent complementary RNAs (cRNAs) with a random priming method of the Arraystar Super RNA Labelling Kit. Labelled cRNAs were then purified using the RNeasy Mini kit (Qiagen GmbH, Hilden, Germany). Labelled cRNA quality and quantity were determined with the NanoDrop ND-1000 spectrophotometer (Agilent Technologies, Santa Clara, USA). Subsequently, the labelled cRNA was fragmented and hybridized onto the Arraystar human circRNA microarray (circular RNA array V2.0 RNA; Arraystar). The hybridized arrays were scanned using an Axon GenePix 4000B microarray scanner (Axon Instruments, Foster City, USA).

Cell culture and proliferation assay

As described previously [5–7], primary hPASMCs were separated from control subjects using distal pulmonary arteries and cultured in high glucose Dulbecco's modified Eagle's medium (DMEM; Biological Industries, Cromwell, USA) containing 10% fetal bovine serum (FBS; Biological Industries), 1% penicillin and streptomycin (Beyotime, shanghai, China) at 37°C. Then, cells at passages 3–8 were used for the *in vitro* experiments.

Cell count kit-8 (CCK-8; Beyotime) was used to evaluate cell proliferation. Briefly, sells were seeded into 24-well plates at a concentration of 1×10^4 cells/well. After treatment, 10 μL CCK-8 solution was added to each well and incubated at 37°C for 2 h. The absorbance at 450 nm was determined with an iMark™ microplate reader (Bio-Rad, Hercules, USA). Cell viability was assessed by MTT assay. Briefly, cells were cultured in 96-well plates and treated with different vectors for 24 h to 72 h. After treatment, 10 μL of 3-(4,5-dimethylthiazol-2-yl)-2,5-diphenyltetrazolium bromide solution (Beyotime) was add to each well and incubated for 4 h at 37°C. After addition of 100 μL DMSO to each well, the absorbance was measured at 570 nm with the iMark™ microplate reader. All experiments were performed in triplicate.

Cell transfection

All small interfering RNA (circ-BPTF-siRNA-1, circ-BPTF-siRNA-2, NC-siRNA and NC-mimics) sequences were purchased from

(Genepharma, Shanghai, China). According to the manufacturer's instructions, a total of 2×10^5 hPASMCs were seeded in a 6-well plate overnight at 37°C. The cells were then cultured in serum-free DMEM medium for 2 h prior to transfection. The cells were subsequently transiently transfected with small interfering RNA and cells were transfected with Lipofectamine 2000 reagent (Invitrogen, Carlsbad, USA). All interference sequences are listed in Table 1.

qRT-PCR

Total RNA was isolated using the TRIzol reagent. cDNA was synthesized using a First-Strand cDNA Synthesis Kit (Invitrogen). The relative mRNA expression was analysed via RT-PCR using SYBR Green qPCR Mix (TransGen Biotech, Beijing, China). PCR conditions were as follows: 95°C for 10 min, 40 cycles of 95°C for 15 s, 60°C for 60 s, 95°C for 15 s, and 60°C for 15 s. A Roche LightCycler 480 Instrument II (Roche, Indianapolis, USA) was used for real-time quantitative fluorescence analysis with a two-step method. *GAPDH* and *U6* nuclear RNA were used as internal controls. The primers used in this study are listed in Table 1.

Luciferase reporter assay

circ-BPTF and CEMIP containing miR-486-5p binding sites were amplified through PCR and cloned into the pmirGLO Dual-Luciferase miRNA Target Expression Vector (Genepharma). Conditions for the PCR were: 95°C, 3 min, 94°C, 30 s, 65°C, 30 s, 72°C, 1 min, and 30 cycles, 72°C, 5 min. The mutation fragment of the 3′-UTR of *CEMIP* or circ-BPTF was inserted into the same sites in the Dual-Luciferase miRNA Target Expression Vector. Cells were cotransfected with miR-486-5p mimics and pmirGLO vector carrying the desired fragment using the Lipofectamine 2000 reagent for 48 h. Luciferase activities were measured by the dual-luciferase reporter assay system (Promega) according to the manufacturer's instructions.

Immunocytochemistry staining

After different treatments, cells in 24-well plates were fixed with 75% alcohol for 5 min and permeabilized with 0.5% Triton X-100 for 5 min. Cells were incubated with primary antibodies against α-smooth muscle actin (1:1000) or PCNA for (1:4000; Abcam) 2 h and subsequent with horseradish peroxidase (HRP)-conjugated goat anti-rabbit IgG (Abcam, Cambridge, USA) for 2 h at room temperature. Immunoreactivity was visualized by using diaminobenzidine (DAB; Beyotime). A negative control was performed using PBS instead of the primary antibodies. Images were obtained using a fluorescence inverted microscope (Olympus, Tokyo, Japan). The relative PCNA level was expressed as the ratio of PCNA-positive cells (brown stained) to the total cell number.

TUNEL assay

After different treatments, cells in 24-well plates were fixed with 75% alcohol. Apoptosis of human PASMCs *in vitro* was evaluated using a TUNEL staining kit (AB66110; Abcam, Cambridge, UK)

Table 1. Sequences of the primers and miRNAs used in this study

Name	Sequence (5′→3′)
hsa_circ_0004893 (F)	GTTGCAGGATTGGGAAGGTT
hsa_circ_0004893 (R)	CAGTCTCGGTGTCCAGGAGT
hsa_circ_0002970 (F)	AGACGAAAGGGGAGGTTATGA
hsa_circ_0002970 (R)	TGCAGGTACATTGGTTTCCC
hsa_circ_0008199 (F)	AGAATAAAGATAACCAAGACAAGAG
hsa_circ_0008199 (R)	TTGCGAAGACACCTGAAGC
hsa_circ_0045462 (circ-BPTF) (F)	CCTGTGATGGTACAGCCAGAAA
hsa_circ_0045462 (circ-BPTF) (R)	TGGTGCTGGTTGTACTGCTTGT
hsa_circ_0045462 siRNA-1 (circ-BPTF-siRNA-1) sense	GAUGGUACAGCCAGAAACGTT
hsa_circ_0045462 siRNA-1 (circ-BPTF-siRNA-1) antisense	CGUUUCUGGCUGUACCAUCTT
hsa_circ_0045462 siRNA-2 (circ-BPTF-siRNA-2) sense	CAGCCAGAAACGACUGGAGTT
hsa_circ_0045462 siRNA-2 (circ-BPTF-siRNA-2) antisense	CUCCAGUCGUUUCUGGCUGTT
Negative control siRNA (NC-siRNA) (sense)	UUCUCCGAACGUGUCACGUTT
Negative control siRNA (NC-siRNA) (antisense)	ACGUGACACGUUCGGAGAATT
Negative control mimics (NC-mimics) (sense)	UUCUCCGAACGUGUCACGUTT
Negative control mimics (NC-mimics) (antisense)	ACGUGACACGUUCGGAGAATT
miR-486-5p sense	GATGCACATCCTGTACTGAGCTG
miR-486-5p antisense	TATGGTTGTTCACGACTCCTTCAC
U6 sense	CTCGCTTCGGCAGCACA
U6 antisense	CTCGCTTCGGCAGCACA
CEMIP sense	CCAGGAATGTTGAATGTCT
CEMIP antisense	ATTGGCTCTTGGTGAATG
GAPDH (F)	AATCCCATCACCATCTTC
GAPDH (R)	AGGCTGTTGTCATACTTC

according to the manufacturer's protocol, and observed under the fluorescence inverted microscope. For the evaluation of TUNEL staining, the number of TUNEL-positive nuclei was counted in 5 randomly selected fields, averaged and expressed as a percentage of labeled nuclei within the fields.

Western blot analysis

Total protein of cells was extracted and determined using Bradford reagent (Bio-Rad). Then, 50 μg of protein was subject to 10% SDS-PAGE. Protein expression were detected by immunoblotting using primary antibodies against CEMIP (1:300; Abcam), cyclin D1 (1:1000; Abcam), and β-actin (1:5000; Santa Cruz). The secondary antibody was the horseradish peroxidase (HRP)-conjugated goat anti-rabbit IgG. A commercial enhanced chemiluminescence kit (Thermo Fisher Scientific, Waltham, USA) was used for immunoreactivity detection. The optical density of the visualized blots was analysed using a gel imaging analysis system (Bio-Rad). The relative density values of each target protein were normalized to GAPDH.

Statistical analysis

Data are expressed as the mean ± standard deviation (SD). For the intergroup comparisons, an unpaired two-tailed Student's *t*-test was applied. For the multigroup comparisons, a one-way ANOVA followed by Tukey's test as the post hoc test was applied. $P < 0.05$ was considered statistically significant.

Results

Clinical data

The baseline characteristics of all subjects are shown in Table 2. There were no differences between the two groups with regard to age and smoking history. As expected from the selected criteria, the forced expiratory volume in 1 second/fixed vital capacity ratio (FEV1/FVC) and forced expiratory volume in 1 second (FEV1% predicted) in COPD patients were significantly lower than those in the control group (FEV1/FVC: 73.65 ± 11.59 vs 94.87 ± 11.13, $P < 0.01$; FEV1% predicted: 60.52 ± 8.75 vs 79.13 ± 7.04, $P < 0.01$). Although no hypoxemia existed in any of the patients who underwent surgery, the partial pressure of arterial oxygen in COPD patients was markedly lower than that in non-COPD patients (69.3 ± 6.2 mmHg vs 82.6 ± 5.2 mmHg, $P < 0.01$). Previous reports and our recent studies demonstrated pulmonary vascular remodelling in early-stage COPD patients [4–7]. In this study, we first evaluated pulmonary vascular remodelling in COPD patients. As shown in Figure 1A,B, the lung tissue that was HE stained in each patient was focused on intermediate vessels (50–500 μm) for

Table 2. Baseline characteristics of all patients

	COPD (*n*=18)	non-COPD (*n*=13)	*P* value
M/F (*n*)	13/5	9/4	0.85
Age (years)	64.20 ± 9.82	57.07 ± 12.18	0.09
Smoker (*n*)	4	2	0.65
FEV1/pred (%)	73.65 ± 11.59	94.87 ± 11.13	<0.01
FEV1/FVC (%)	60.52 ± 8.75	79.13 ± 7.04	<0.01
PaO_2 (mmHg)	69.3 ± 6.2	82.6 ± 5.2	<0.01

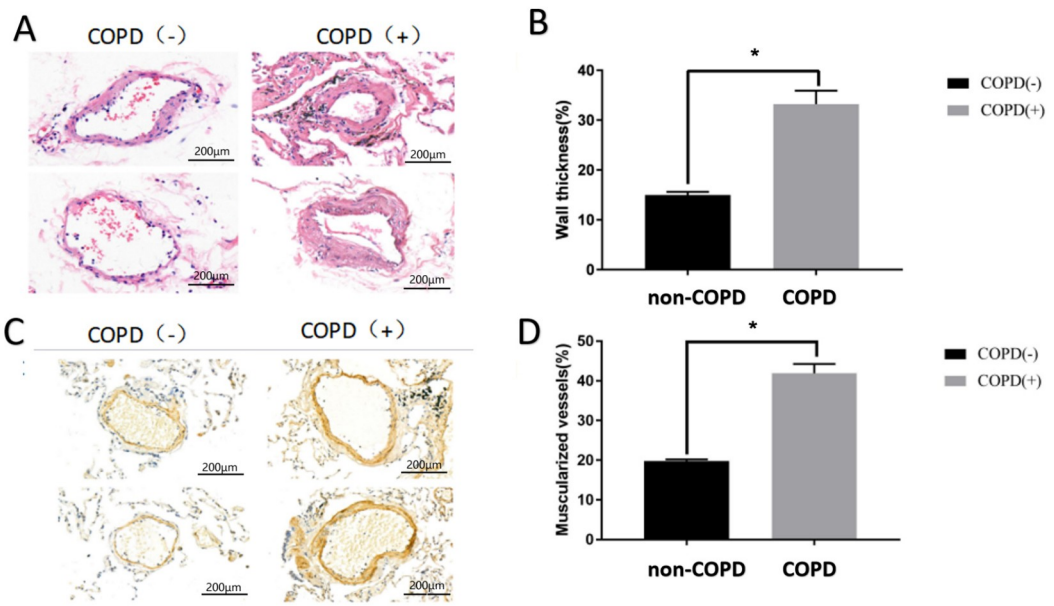

Figure 1. Pulmonary vascular remodelling in COPD patients Lung tissues were collected from COPD or non-COPD patients, and pulmonary vascular remodelling was estimated. (A,B) HE staining showed the wall thickness of pulmonary vessels in patients. (C,D) Immunohistochemistry staining (α-SMA) showed the muscularized vessels of pulmonary vessels in patients. *$P < 0.05$.

evaluating pulmonary vascular remodelling. The pulmonary vascular wall thickness and muscularized vessel ratio in COPD patients were both significantly higher than those in non-COPD patients (Figure 1C,D). These data indicated that COPD patients with the lower partial pressure of arterial oxygen are more likely to have pulmonary arterial remodeling.

circ-BPTF is upregulated in the lungs of COPD patients

To determine the involvement of circRNAs in the progression of COPD, we screened 3610 expressed circRNAs by high-throughput transcriptome sequencing of pulmonary arterial explants in lung tissues from COPD patients or controls and found 48 differentially expressed circRNAs with changes of more than 2 folds. Overall, 26 of these circRNAs were significantly upregulated, and 22 were significantly downregulated. We selected 4 significantly upregulated circRNAs and further verified the expressions of these circRNAs by quantitative polymerase chain reaction (qPCR) using pulmonary arterial smooth muscle strips from lung tissues of COPD patients or controls (Figure 2A–E). Our results showed that circ-BPTF was the most significantly elevated circRNA, consistent with the sequencing results. We then chose circ-BPTF for subsequent analyses. Additionally, we performed fluorescence *in situ* hybridization analysis to determine the distribution of circ-BPTF and found that circ-BPTF was mainly localized in pulmonary arteries (Figure 2F). These data indicated that circ-BPTF may play vital roles in the regulation of COPD.

circ-BPTF promotes hPASMC proliferation

In order to investigated the function of circ-BPTF in the pathogenesis of *COPD*, we analyzed the role of circ-BPTF in pulmonary arterial smooth muscle cell proliferation under hypoxic conditions. Hypoxia induced circ-BPTF upregulation in hPASMCs *in vitro* in a time-dependent manner (Figure 3A). Specific siRNA targeting circ-BPTF significantly inhibited the mRNA level of circ-BPTF in hPASMCs exposed to hypoxia, and we found that siRNA-1 had the most obvious effects (Figure 3B). Therefore, we transfected hPASMCs with siRNA-1 to study the function of circ-BPTF. As shown in Figure 3C, the CCK-8 results indicated that hypoxia induced cell proliferation in a time-dependent manner. However, siRNA targeting circ-BPTF significantly inhibited proliferation in hypoxia-exposed cells. These results were also confirmed by MTT assay (Figure 3D). Next, we transfected PASMCs with a circ-BPTF-overexpressing vector. As shown in Figure 3E,F, circ-BPTF overexpression significantly promoted cell proliferation. Overexpression of circ-BPTF also increased the percentage of PCNA-positive PASMCs (Figure 3G,H). The immunocytochemistry staining showed that hypoxia-induced PCNA overexpression was reversed by knockdown of *circ-BPTF* following transfection of PASMCs with circ-BPTF siRNA (Figure 3J,K). Additionally, hypoxia decreased the percentage of TUNEL-positive cells, which was also reversed by knockdown of *circ-BPTF* (Figure 3J,K). These data suggested that circ-BPTF promotes hPASMC proliferation.

circ-BPTF is a molecular sponge for miR-486-5p

circRNAs act as a competitive endogenous sponges for miRNAs. We speculated that circ-BPTF might serve as a molecular sponge to promote PASMC proliferation. Using the bioinformatics software miRanda and RNAhybrid, we predicted that circ-BPTF may sponge miR-202-3p, miR-758-3p, miR-486-5p and miR-218-5p (Figure 4A). qPCR results showed that miR-486-5p level was downregulated, but miR-202-3p level were upregulated after exposure to hypoxia, (Figure 4B). There were no significant differences in miR-218-5p and miR-758-3p levels between normoxic cells and hypoxic cells. Moreover, a recent report demonstrated the downregulation of miR-486-5p in PASMCs [21]. Therefore, we focused on miR-486-5p in subsequent analyses. We predicted that there are 2 binding sites

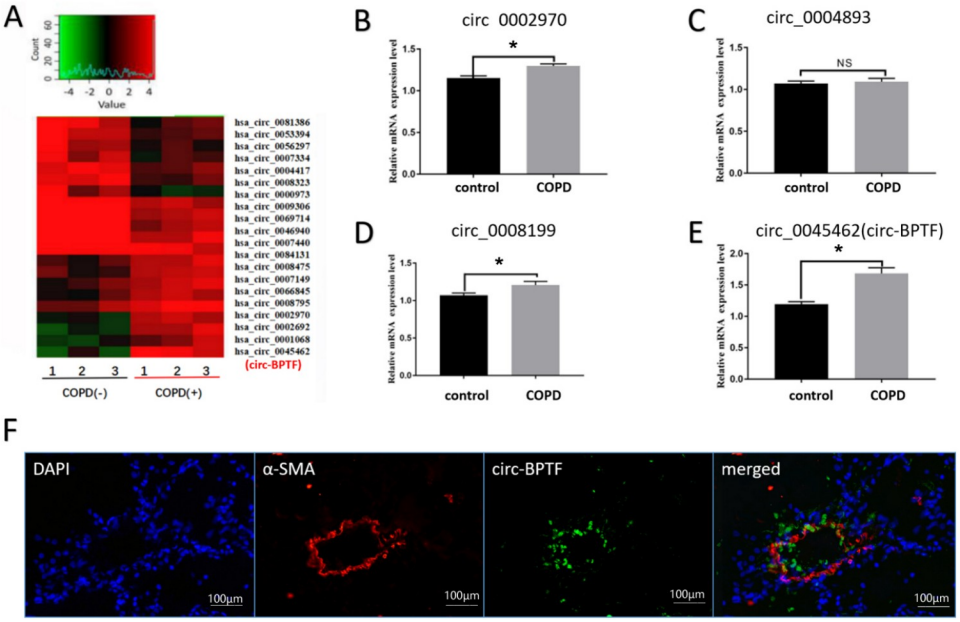

Figure 2. circ-BPTF is upregulated in the lung and smooth muscle of COPD patients Lung tissues were collected from COPD or control patients. Total RNA was isolated, and circRNA microarray hybridization was performed based on Arraystar's standard protocols. (A) Heatmap and volcano map analysis of circular RNAs in lung tissues from COPD patients and controls. (B-E) qPCR analysis of the expressions of four circRNAs in lung tissues from COPD patients and controls (n = 6). (F) Fluorescence *in situ* hybridization of circ-BPTF in lung tissues from COPD patients. *$P < 0.05$.

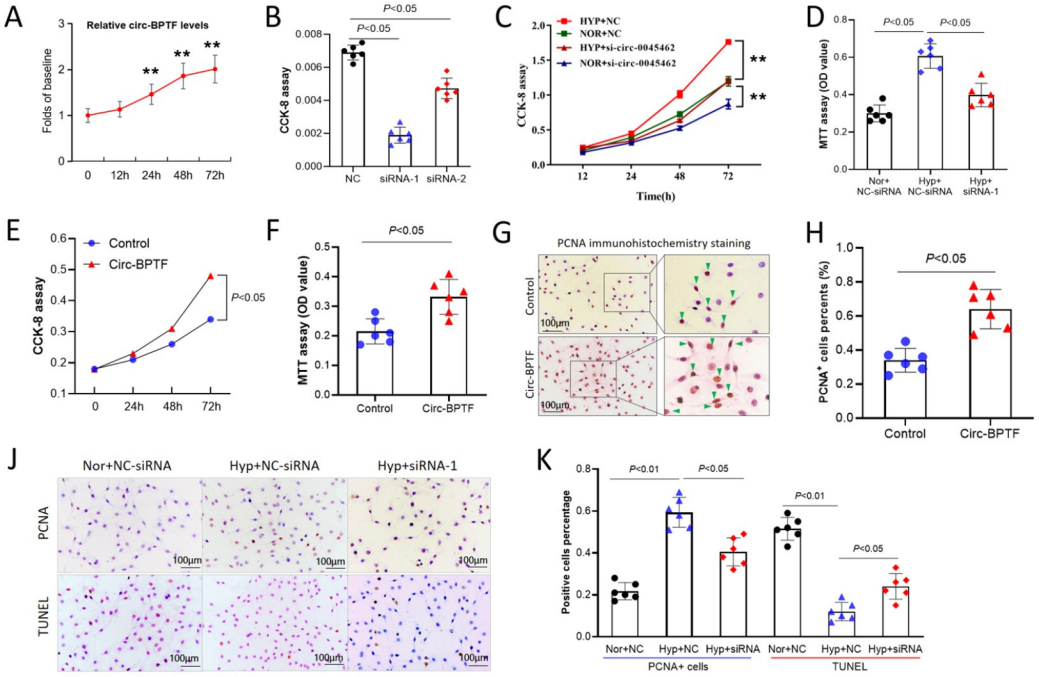

Figure 3. circ-BPTF promotes PASMC proliferation Human PASMCs were cultured *in vitro* under hypoxia or normoxia. Specific siRNA was used to knockdown *circ-BPTF*. An overexpression vector was used for overexpression of circ-BPTF. (A) qPCR analysis of circ-BPTF levels after exposure to hypoxia for different time. (B) Specific siRNA knockdown of *circ-BPTF* in hypoxia-exposed PASMCs. (C–D) CCK-8 and MTT assays showed that circ-BPTF-specific siRNA suppressed cell proliferation in hypoxia-exposed PASMCs. (E–F) CCK-8 and MTT assays showed that circ-BPTF overexpression promoted PASMC proliferation. (G–H) circ-BPTF overexpression increased the percentage of PCNA-positive cells. (J–K) Immunohistochemistry staining and the TUNEL assay showed that circ-BPTF-specific siRNA suppressed PCNA-positive cells and increased TUNEL-positive cells in hypoxia-exposed PASMCs. $^{**}P < 0.01$.

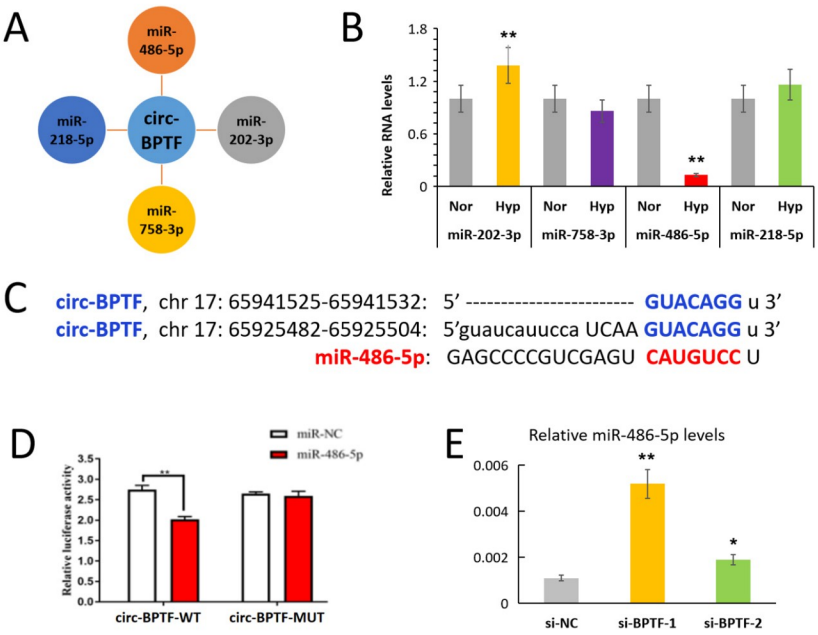

Figure 4. circ-BPTF sponges miR-486-5p (A) Bioinformatics software (miRanda and RNAhybrid) predicted miRNAs that could bind to circ-BPTF. (B) Human PASMCs were exposed to hypoxia for 24 h, and qPCR was used to detect miR-202-3p, miR-758-3p, miR-486-5p and miR-218-5p expression levels. (C) The predicted binding sites of circ-BPTF and miR-486-5p by TargetScan. (D) Dual luciferase reporter assays demonstrated the interactions between circ-BPTF and miR-486-5p. (E) Human PASMCs were transfected with circ-BPTF-specific siRNA (si-BPTF) or negative control siRNA (si-NC) before exposure to hypoxia for 24 h. qPCR was used to detect miR-486-5p level. $^{*}P < 0.05$, $^{**}P < 0.01$.

between circ-BPTF and miR-486-5p by TargetScan analysis (Figure 4C). Next, we used a dual luciferase vector plasmid system to verify whether circ-BPTF binds to miR-486-5p. We found that the ratio of luciferase for wild-type circ-BPTF was significantly decreased when compared with that of the negative control after miR-486-5p exposure (Figure 4D). However, the ratio of luciferase for mutant circ-BPTF did not change compared with the negative control after miR-486-5p exposure. Moreover, circ-BPTF-specific siRNA significantly reversed the suppression of circ-BPTF on miR-486-5p expression (Figure 4E). These results indicated that circ-BPTF is a molecular sponge for miR-486-5p.

circ-BPTF regulates cell proliferation by sponging miR-486-5p

To identify the role of miR-486-5p in cell proliferation, PASMCs were transfected with miR-486-5p mimics and exposed to hypoxia for 24-72 hours. The CCK-8 results showed that miR-486-5p mimics significantly inhibited hypoxia-induced cell proliferation (Figure 5A). The PCNA-positive cells were also significantly decreased by miR-486-5p transfection, as shown by immunocytochemistry staining (Figure 5B, C). Additionally, miR-486-5p mimics increased the percentage of TUNEL-positive cells (Figure 5B,C). Next, we used rescue experiments to identify whether circ-BPTF promotes cell proliferation by sponging miR-486-5p. We cotransfected PASCMCs with circ-BPTF siRNA and miR-486-5p inhibitors before exposure to hypoxia. The results of the EdU assays showed that both circ-BPTF siRNA and miR-486-5p mimics inhibited hypoxia-induced cell proliferation, whereas the miR-486-5p inhibitor reversed the inhibitory effect of circ-BPTF siRNA on cell proliferation (Figure 5D,E). These results demonstrated that circ-BPTF could regulate PASCMC proliferation by sponging miR-486-5p.

miR-486-5p targets CEMIP in PASMCs exposed to hypoxia

Previous reports have demonstrated that cell migration-inducing protein (CEMIP) is a downstream target protein of miR-486-5p [22,23]. We next attempted to identify the regulatory role of miR-486-5p in CEMIP expression in PASMCs. Using the bioinformatics software miRanda and TargetScanHuman, we predicted two putative binding sites for miR-486-5p on the 3′-UTR of CEMIP mRNA (Figure 6A). The results of dual luciferase reporter assay showed that the ratio of luciferase for wild-type CEMIP was significantly decreased compared with that of the negative control after miR-486-5p mimic exposure (Figure 6B). However, the ratio of luciferase for mutant CEMIP did not change compared with the negative control after miR-486-5p mimic exposure. These results indicated that miR-486-5p could regulate CEMIP expression. Next, we explored the regulatory role of miR-486-5p in CEMIP expression. As shown in Figure 6C, miR-486-5p mimics markedly suppressed the mRNA level of CEMIP in human PASMCs after hypoxia exposure. Furthermore, miR-486-5p mimics significantly inhibited CEMIP protein level, while miR-486-5p inhibitor increased CEMIP protein level (Figure 6D,E). These results indicated that CEMIP might be a target of miR-486-5p in hypoxia-induced PASMC proliferation.

CEMIP promotes cell proliferation in PASMCs exposed to hypoxia

Subsequently, we tried to uncover the role of CEMIP in hypoxia-induced PASMC proliferation. Figure 7A shows the data from the GEO database (GSE56698). A microarray study of lung homo-

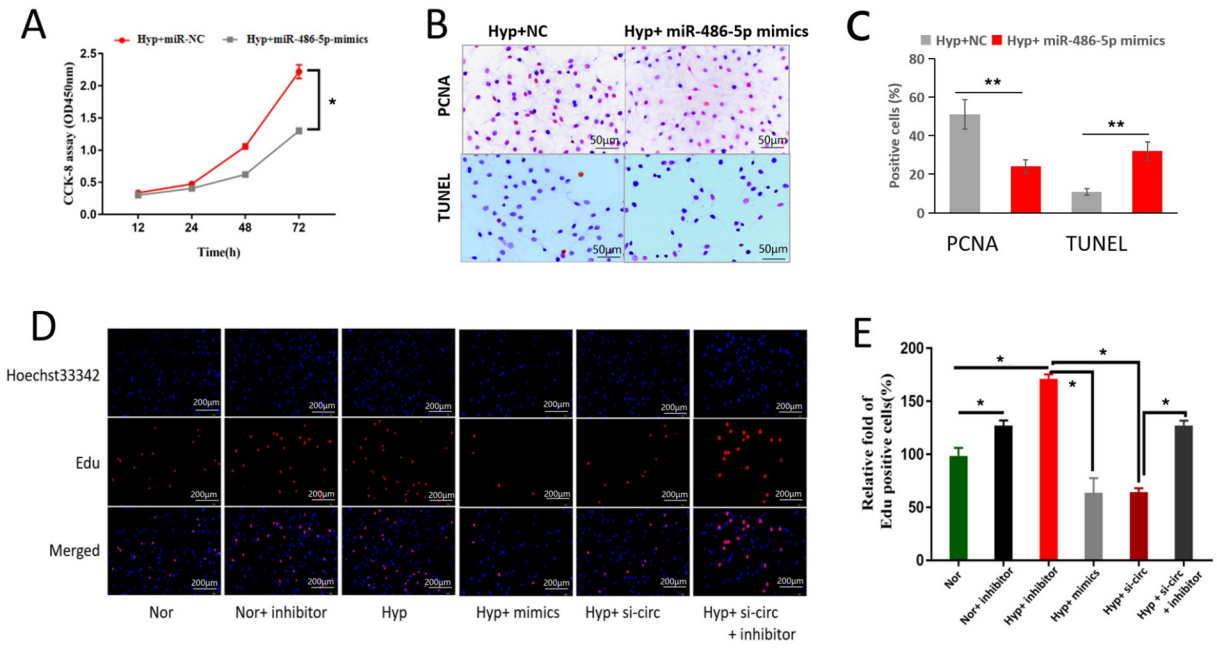

Figure 5. circ-BPTF regulates cell proliferation by sponging miR-486-5p Human PASMCs were cultured *in vitro* under hypoxia or normoxia. Cells were transfected with miR-486-5p mimic, miR-486-5p inhibitor or circ-BPTF-specific siRNA. (A) CCK-8 assay showed that miR-486-5p mimic inhibited proliferation of hypoxic cells. (B,C) Immunohistochemistry staining and the TUNEL assay showed that miR-486-5p mimic suppressed the percentage of PCNA-positive cells but increased the percentage of TUNEL-positive cells. (D,E) Immunofluorescence staining for the EdU assay showed that both circ-BPTF siRNA and miR-486-5p mimic decreased the percentage of hypoxia-induced Edu-positive cells, whereas the miR-486-5p inhibitor reversed this inhibitory effect. Inhibitor: miR-486-5p inhibitor; mimic: miR-486-5p mimic; sic-circ: circ-BPTF specific siRNA. $*P<0.05$, $**P<0.01$.

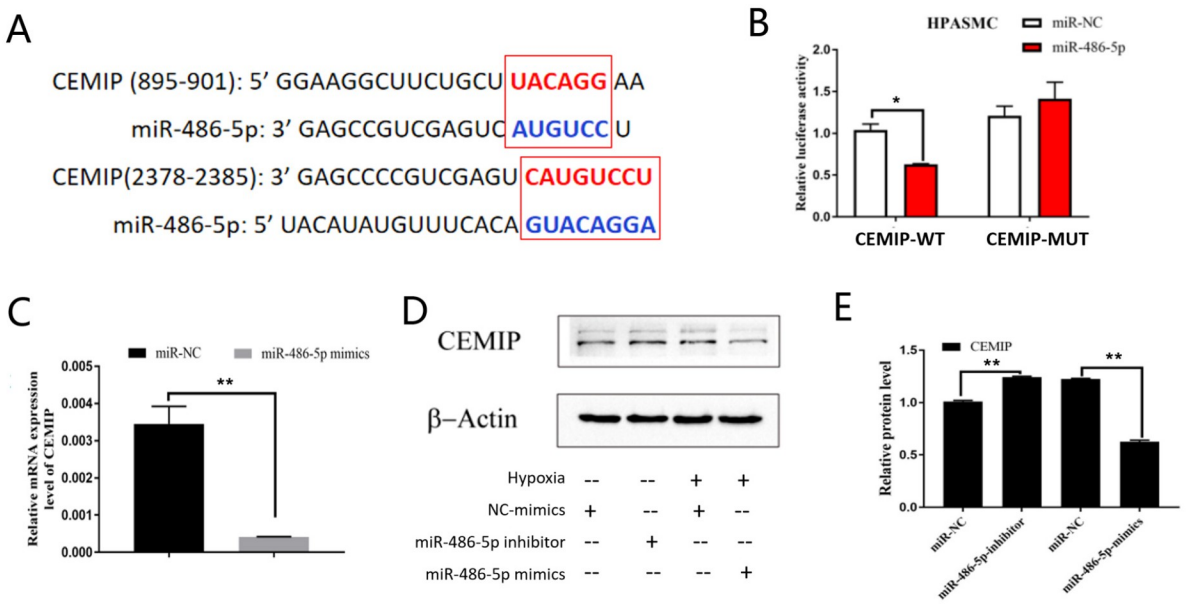

Figure 6. miR-486-5p targets CEMIP (A) TargetScan predicted the binding sites between miR-486-5p and CEMIP. (B) Dual luciferase reporter assay was used to identify the interaction between miR-486-5p and CEMIP. (C) qPCR showed that miR-486-5p mimic inhibited CEMIP expression in hypoxic PASMCs. (D,E) Western blot analysis results verified that the miR-486-5p inhibitor upregulated CEMIP protein level, but the miR-486-5p mimic downregulated CEMIP protein level. $*P<0.05$, $**P<0.01$.

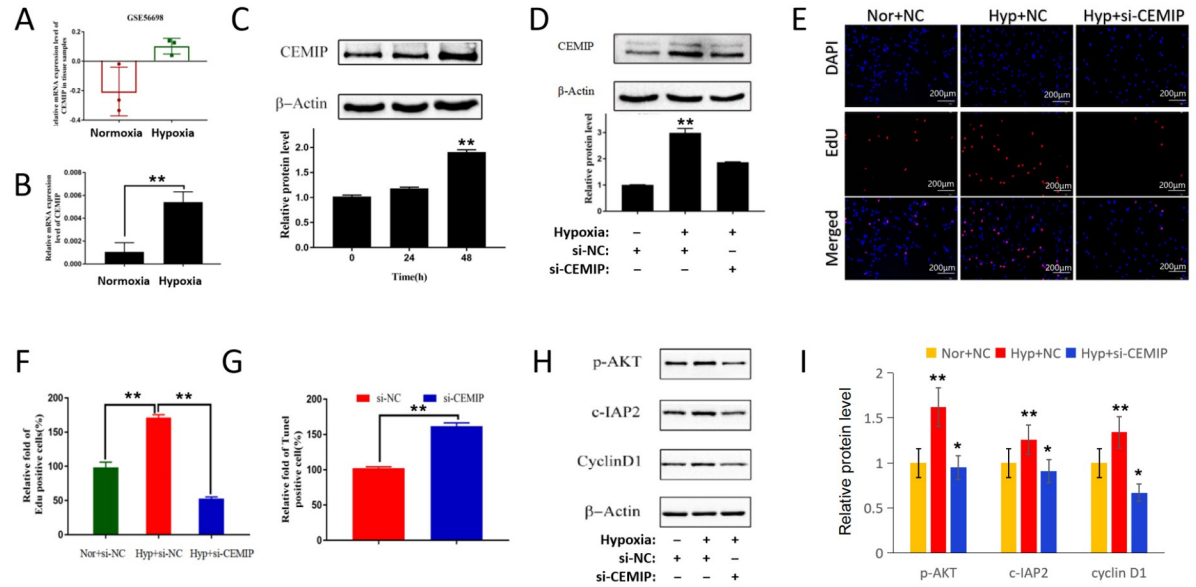

Figure 7. CEMIP promotes the proliferation of PASMCs exposed to hypoxia Human PASMCs were cultured *in vitro* under hypoxia or normoxia. Cells were transfected with CEMIP-specific siRNA or negative control siRNA. (A) A microarray study of lung homogenates from the GEO database (GSE56698) showed the upregulation of CEMIP in hypoxic mice. (B) qPCR was used to detect the CEMIP mRNA level in hypoxic PASMCs. (C) Western blot analysis results showed a time-dependent upregulation of CEMIP protein level in hypoxic PASMCs. (D) Specific siRNA (si-CEMIP) suppressed CEMIP protein expression in hypoxic PASMCs. (E,F) Immunofluorescence staining for the EdU assay showed that si-CEMIP inhibited the percentage of EdU-positive cells in hypoxic PASMCs. (G) TUNNEL assay showed that si-CEMIP increased the percentage of TUNNEL-positive cells in hypoxic PASMCs. (H,I) si-CEMIP inhibited the downstream targets in hypoxic PASMCs. $*P<0.05$, $**P<0.01$.

genates revealed that CEMIP is highly upregulated in hypoxic mice compared with that in control mice. Next, we examined CEMIP expression in human PASMCs. As shown in Figure 7B, C, hypoxia exposure not only increased CEMIP mRNA level but also increased CEMIP protein level. Moreover, hypoxia increased CEMIP expression in a time-dependent manner (Figure 7C). Then, we used CEMIP-specific siRNA to knockdown its expression. In PASMCs exposed to hypoxia, specific siRNA significantly inhibited CEMIP expression (Figure 7D). Although hypoxia increased the Edu-positive cell percentage, CEMIP-specific siRNA significantly reversed this increase compared with the negative control siRNA (Figure 7E,F). In contrast, CEMIP-specific siRNA increased the

number of TUNEL-positive cells in hypoxia-exposed PASMCs (Figure 7G). Additionally, CEMIP-specific siRNA inhibited the protein expressions of p-AKT, cyclin D1 and cIAP2 (Figure 7H,I). These results showed that CEMIP might promote PASMC proliferation via the p-AKT, cyclin D1 and cIAP2 pathways after hypoxia exposure.

circ-BPTF regulates the miR-486-5p/CEMIP axis

To identify the regulatory effect of circ-BPTF on the miR-486-5p/CEMIP axis, we cotransfected PASMCs with circ-BPTF siRNA and miR-486-5p mimic or inhibitor before exposure to hypoxia in the rescue experiments. Western blot analysis results showed that contransfection with circ-BPTF-specific siRNA and miR-486-5p mimic inhibited hypoxia-induced CEMIP protein upregulation. However, miR-486-5p inhibitor reversed the inhibitory effect of circ-BPTF-specific siRNA on CEMIP protein expression (Figure 8A,B). circ-BPTF-specific siRNA suppressed not only CEMIP expression but also the expression of its downstream target, p-AKT (Figure 8C, D). These results demonstrated the role of the circ-BPTF/miR-486-5p/CEMIP axis in regulating hypoxia-induced PASMC proliferation.

Discussion

In this study, we identified a novel circRNA, circ-BPTF, and demonstrated the role of the circ-BPTF/miR-486-5p/CEMIP axis in regulating hypoxia-induced PASMC proliferation. Although circRNAs have been implicated in cancers, only a few reports focused on the role of circRNAs in COPD. This study provided more evidence about the role of circRNAs in PASMC proliferation and pulmonary vascular remodelling in COPD.

Although some reports have proven the role of circRNAs in cardiovascular disorders and pulmonary hypertension, few studies focused on the role of circRNAs in COPD-associated pulmonary vascular remodelling [24–26]. In this study, we used microarray analysis to identify changes in circRNA profiles in lung tissues of COPD patients and in PASMCs exposed to hypoxia. We indentified a novel circRNA, circ-BPTF, and demonstrated the potential mechanism of circ-BPTF in pulmonary vascular remodelling of COPD by promoting PASMC proliferation via regulating target miRNAs and downstream proteins. As a new class of noncoding RNA molecules, circRNAs are protected from degradation and have greater stability than linear RNAs. Numerous circRNAs are expressed in a disease-specific manner. Furthermore, due to other features of circRNAs (including stability, conservation and high abundance in body fluids), they are believed to be potential biomarkers for various diseases. Our study proved a novel circRNA which is specific to COPD-associated pulmonary vascular remodelling. This might provide evidence that circRNAs may be potential biomarkers.

As a molecular sponges of miRNAs, circRNAs act by securing the target miRNA-mediated suppression of downstream proteins [27,28]. In this study, we used bioinformatics analysis to predict miRNAs that may bind to circ-BPTF and verified that miR-486-5p could be sponged by circ-BPTF via binding sites at positions 525-532 and 485-504 of circ-BPTF. We further revealed that circ-BPTF promoted PASMC proliferation by sponging miR-486-5p. This result is consistent with other reports on the roles of circRNAs in pulmonary hypertension [16–20], and suggests a circRNA/miRNA pathway underlying PASMC proliferation and pulmonary vascular remodelling in COPD patients.

Many previous studies have indicated that miR-486-5p regulates the proliferation of many kinds of cancer cells [21,29,30,22]. However, no reports focused on the role of miR-486-5p in regulating hypoxic PASMC proliferation. Our reports first revealed that miR-

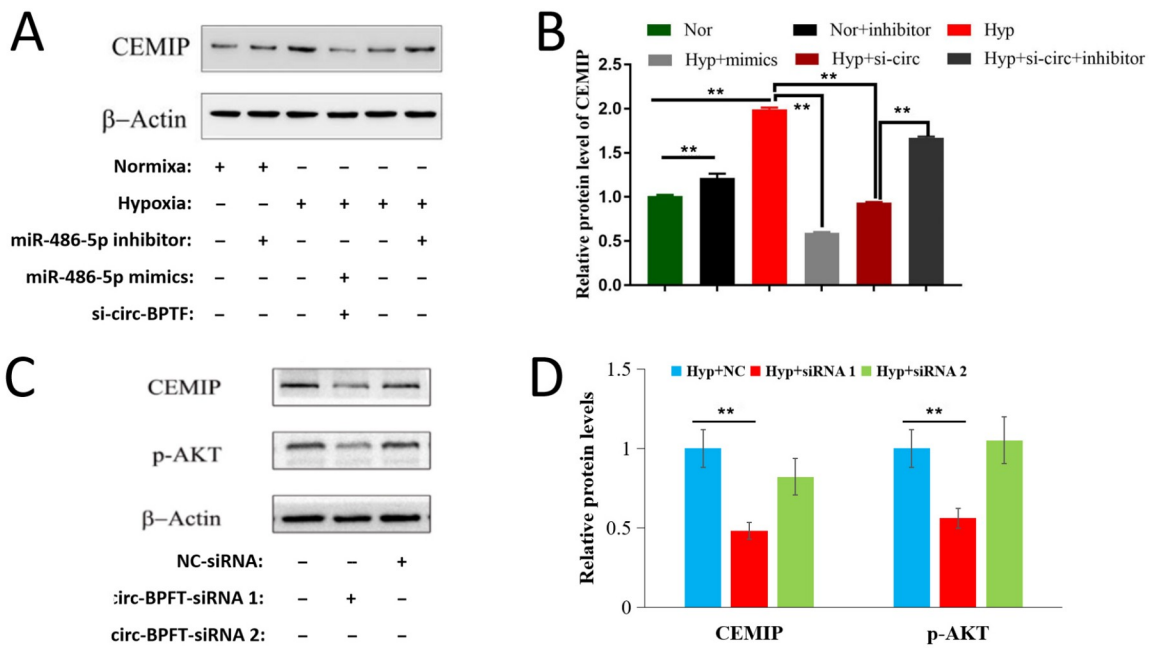

Figure 8. circ-BPTF regulates the miR-486-5p/CEMIP axis Human PASMCs were cultured *in vitro* under hypoxia or normoxia. Cells were cotransfected with miR-486-5p mimic or miR-486-5p inhibitor and circ-BPTF-specific siRNA. (A,B) Western blot analysis results showed the effect of miR-486-5p mimic, miR-486-5p inhibitor and circ-BPTF-specific siRNA on CEMIP protein level under hypoxia or normoxia. circ-BPTF-specific siRNA and miR-486-5p mimic inhibited CEMIP protein level in hypoxic PASMCs, but miR-486-5p inhibitor reversed this inhibitory effect. (C,D) Western blot analysis results showed the inhibitory effect of circ-BPTF-specific siRNA on CEMIP protein level and its downstream targets in hypoxic PASMCs. $^{**}P < 0.01$.

486-5p inhibits cell proliferation in hypoxia-exposed PASMCs. Moreover, we identified that the circ-BPTF/miR-486-5p pathway is involved in promoting PASMC proliferation under hypoxic conditions. miRNAs are small noncoding RNAs involved in the regulation of posttranscriptional gene expression [31]. miRNA dysregulation has been reported to promote the development of various diseases, including cancers [32]. Indeed, impairment of miRNA expression has been shown to be involved in vascular cell remodelling processes, such as adventitial fibroblast migration, PASMC proliferation and pulmonary arterial endothelial cell dysfunction [33]. This study demonstrated the mechanisms through which a novel circRNA (circ-BPTF) regulates hypoxic PASMC proliferation and pulmonary vascular remodelling in COPD by sponging miR-486-5p. This might enrich our understanding of the mechanism underlying COPD-associated pulmonary vascular remodelling or pulmonary hypertension.

By inhibiting downstream target genes, miRNAs exert pathophysiological functions in multiple physiological and pathological processes [34]. Bioinformatics analysis in this study showed that CEMIP is a target of miR-486-5p. Although other reports indicated that CEMIP plays a critical role in tumor development and cell proliferation, its role in PASMC proliferation and vascular remodelling in COPD remains unclear [23,35]. This study first showed that the miR-486-5p/CEMIP axis regulates PASMC proliferation under hypoxic conditions, providing a new potential diagnostic and therapeutic target for this disease. Our previous studies demonstrated that cyclin D1 participates in pulmonary vascular remodelling in COPD and pulmonary hypertension [5–7]. Although some pathways might be involved in this process, such as cyclin D1 and p-AKT, it is unclear whether this mechanism participates in pulmonary vascular remodelling in COPD or pulmonary hypertension. In this report, we preliminarily showed that cyclin D1, p-AKT and c-IAP2 might be the downstream targets of CEMIP in PASMC proliferation. Further studies are needed to determine the roles of CEMIP and its downstream mechanism in pulmonary vascular remodelling.

In summary, our findings indicated that hypoxia upregulates circ-BPTF. This change results in the promotion of PASMC proliferation by sponging miR-486-5p, which targets CEMIP. Thus, we identified a novel circRNA and elucidated the function and mechanisms of this circRNA in PASMCs and pulmonary vascular remodelling in COPD. Future studies are needed to confirm these findings and to provide additional insights into the promising applications of this circRNA.

Funding

This work was supported by the grants from the Suzhou Municipal Application Basic Research Project (SYS2019047), the Program of Key Talents of Medical Science in Jiangsu Province (QNRC2016745), and the National Nature Science Foundation of China (No. 81970051).

Conflict of Interest

The authors declare that they have no conflict of interest.

References

1. Nathan SD, Barbera JA, Gaine SP, Harari S, Martinez FJ, Olschewski H, Olsson KM, *et al.* Pulmonary hypertension in chronic lung disease and hypoxia. *Eur Respir J* 2019, 53: 1801914
2. Lei Y, Yang Q, Nie Y, Wan J, Deng M. Small-molecule inhibitor LF3 restrains the development of pulmonary hypertension through the Wnt/β-catenin pathway. *Acta Biochim Biophys Sin* 2021, 53: 1277–1289
3. Li C, Liu P, Song R, Zhang Y, Lei S, Wu S. Immune cells and autoantibodies in pulmonary arterial hypertension. *Acta Biochim Biophys Sin* 2017, 49: 1047–1057
4. Churg A, Cosio M, Wright JL. Mechanisms of cigarette smoke-induced COPD: insights from animal models. *Am J Physiol Lung Cell Mol Physiol* 2008, 294: L612–L631
5. Zeng D, Liu X, Xu Y, Wang R, Xiang M, Xiong W, Ni W, *et al.* Plasmid-based short hairpin RNA against cyclin D1 attenuated pulmonary vascular remodeling in smoking rats. *Microvascular Res* 2010, 80: 116–122
6. Wang C, Li C, Lei W, Jiang JH, Huang J, Zeng D. The association of neuron-derived orphan receptor 1 with pulmonary vascular remodeling in COPD patients. *COPD* 2018, 13: 1177–1186
7. Liu Y, Zhang W, Wang C, Huang J, Jiang J, Zeng D. Resveratrol prevented experimental pulmonary vascular remodeling via miR-638 regulating NR4A3/cyclin D1 pathway. *Microvascular Res* 2020, 130: 103988
8. Zeng D, Xu G, Lei W, Wang R, Wang C, Huang J. Suppression of cyclin D1 by plasmid-based short hairpin RNA ameliorated experimental pulmonary vascular remodeling. *Microvascular Res* 2013, 90: 144–149
9. Wang CG, Lei W, Li C, Zeng DX, Huang JA. Neuron-derived orphan receptor 1 promoted human pulmonary artery smooth muscle cells proliferation. *Exp Lung Res* 2015, 41: 208–215
10. Bunel V, Guyard A, Dauriat G, Danel C, Montani D, Gauvain C, Thabut G, *et al.* Pulmonary arterial histologic lesions in patients with COPD with severe pulmonary hypertension. *Chest* 2019, 156: 33–44
11. Pichl A, Sommer N, Bednorz M, Seimetz M, Hadzic S, Kuhnert S, Kraut S, *et al.* Riociguat for treatment of pulmonary hypertension in COPD: a translational study. *Eur Respir J* 2019, 53: 1802445
12. Blanco I, Piccari L, Barberà JA. Pulmonary vasculature in COPD: The silent component. *Respirology* 2016, 21: 984–994
13. de Jesus Perez VA. Molecular pathogenesis and current pathology of pulmonary hypertension. *Heart Fail Rev* 2016, 21: 239–257
14. Wang J, Zhu M, Pan J, Chen C, Xia S, Song Y. Circular RNAs: a rising star in respiratory diseases. *Respir Res* 2019, 20: 3
15. Bonnet S, Boucherat O, Paulin R, Wu D, Hindmarch CCT, Archer SL, Song R, *et al.* Clinical value of non-coding RNAs in cardiovascular, pulmonary, and muscle diseases. *Am J Physiol Cell Physiol* 2020, 318: C1–C28
16. Zhang J, Li Y, Qi J, Yu X, Ren H, Zhao X, Xin W, *et al.* Circ-*calm4* Serves as an *miR-337-3p* sponge to regulate Myo10 (Myosin 10) and promote pulmonary artery smooth muscle proliferation. *Hypertension* 2020, 75: 668–679
17. Zhou S, Jiang H, Li M, Wu P, Sun L, Liu Y, Zhu K, *et al.* Circular RNA hsa_circ_0016070 is associated with pulmonary arterial hypertension by promoting PASMC proliferation. *Mol Ther Nucleic Acids* 2019, 18: 275–284
18. Ma C, Gu R, Wang X, He S, Bai J, Zhang L, Zhang J, *et al.* mmu_circ_0000790 is involved in pulmonary vascular remodelling in mice with HPH via microRNA-374c-mediated FOXC1. *Mol Ther Nucleic Acids* 2020, 22: 530–541
19. Jin X, Xu Y, Guo M, Sun Y, Ding J, Li L, Zheng X, *et al.* hsa_circNFXL1_009 modulates apoptosis, proliferation, migration, and potassium channel activation in pulmonary hypertension. *Mol Ther Nucleic Acids* 2020, 23: 1007–1019
20. Guo H, Liu Z. Up-regulation of circRNA_0068481 promotes right ventricular hypertrophy in PAH patients via regulating miR-646/miR-570/miR-885. *J Cell Mol Med* 2021, 25: 3735–3743
21. Heo J, Yang HC, Rhee WJ, Kang H. Vascular smooth muscle cell-derived exosomal microRNAs regulate endothelial cell migration Under PDGF

stimulation. *Cells* 2020, 9: 639
22. Wang J, Tian X, Han R, Zhang X, Wang X, Shen H, Xue L, ***et al.*** Downregulation of miR-486-5p contributes to tumor progression and metastasis by targeting protumorigenic ARHGAP5 in lung cancer. *Oncogene* 2014, 33: 1181–1189
23. Deroyer C, Charlier E, Neuville S, Malaise O, Gillet P, Kurth W, Chariot A, ***et al.*** CEMIP (KIAA1199) induces a fibrosis-like process in osteoarthritic chondrocytes. *Cell Death Dis* 2019, 10: 103
24. Yang L, Liang H, Meng X, Shen L, Guan Z, Hei B, Yu H, ***et al.*** mmu_circ_0000790 is involved in pulmonary vascular remodeling in mice with HPH via microRNA-374c-mediated FOXC1. *Mol Ther Nucleic Acids* 2020, 20: 292–307
25. Jiang Y, Liu H, Yu H, Zhou Y, Zhang J, Xin W, Li Y, ***et al.*** Circular RNA calm4 regulates hypoxia-induced pulmonary arterial smooth muscle cells pyroptosis via the circ-calm4/miR-124-3p/PDCD6 axis. *Arterioscler Thromb Vasc Biol* 2021, 41: 1675–1693
26. Aufiero S, Reckman YJ, Pinto YM, Creemers EE. Circular RNAs open a new chapter in cardiovascular biology. *Nat Rev Cardiol* 2019, 16: 503–514
27. Boon RA, Jaé N, Holdt L, Dimmeler S. Long noncoding RNAs. *J Am College Cardiol* 2016, 67: 1214–1226
28. Jaé N, Dimmeler S. Noncoding RNAs in vascular diseases. *Circ Res* 2020, 126: 1127–1145
29. Kong Y, Li Y, Luo Y, Zhu J, Zheng H, Gao B, Guo X, ***et al.*** circNFIB1 inhibits lymphangiogenesis and lymphatic metastasis via the miR-486-5p/PIK3R1/VEGF-C axis in pancreatic cancer. *Mol Cancer* 2020, 19: 82
30. Hanna JA, Garcia MR, Lardennois A, Leavey PJ, Maglic D, Fagnan A, Go JC, ***et al.*** PAX3-FOXO1 drives miR-486-5p and represses miR-221 contributing to pathogenesis of alveolar rhabdomyosarcoma. *Oncogene* 2018, 37: 1991–2007
31. Negi V, Chan SY. Discerning functional hierarchies of microRNAs in pulmonary hypertension. *JCI Insight* 2017, 2: e91327
32. Boateng E, Krauss-Etschmann S. miRNAs in lung development and diseases. *Int J Mol Sci* 2020, 21: 2765
33. Zhou G, Chen T, Raj JU. MicroRNAs in pulmonary arterial hypertension. *Am J Respir Cell Mol Biol* 2015, 52: 139–151
34. Jusic A, Devaux Y. Noncoding RNAs in hypertension. *Hypertension* 2019, 74: 477–492
35. Rodrigues G, Hoshino A, Kenific CM, Matei IR, Steiner L, Freitas D, Kim HS, ***et al.*** Tumour exosomal CEMIP protein promotes cancer cell colonization in brain metastasis. *Nat Cell Biol* 2019, 21: 1403–1412